ACS APPLIED MATERIALS & INTERFACES

Research Article

www.acsami.org

Multifunctional Cyclotriphosphazene/Hexagonal Boron Nitride Hybrids and Their Flame Retarding Bismaleimide Resins with High Thermal Conductivity and Thermal Stability

Wenqin Jin, Li Yuan, Guozheng Liang,* and Aijuan Gu*

Jiangsu Key Laboratory of Advanced Functional Polymer Design and Application, Department of Materials Science and Engineering College of Chemistry, Chemical Engineering and Materials Science, Soochow University, Suzhou, Jiangsu 215123, China

Supporting Information

ABSTRACT: A novel hybridized multifunctional filler (CPBN), cyclotriphosphazene/hexagonal boron nitride (hBN) hybrid, was synthesized by chemically coating hBN with hexachlorocyclotriphosphazene and p-phenylenediamine, its structure was systemically characterized. Besides, CPBN was used to develop new flame retarding bismaleimide/*o*,*o*′-diallylbisphenol A (BD) resins with simultaneously high thermal conductivity and thermal stability. The nature of CPBN has a strong influence on the flame behavior of the composites. With the addition of only 5 wt % CPBN to BD resin, the thermal conductivity increases 2 times; meanwhile the flame retardancy of BD resin is remarkably increased, reflected by the increased limited oxygen index, much longer time to ignition, significantly reduced heat release rate. The thermogravimetric kinetics, structures of chars and pyrolysis gases, and cone calorimeter tests were investigated to reveal the unique flame retarding mechanism of CPBN/BD composites. CPBN provides multieffects on improving the flame retardancy, especially in forming a protective char layer, which means a more thermally stable and condensed barrier for heat and mass transfer, and thus protecting the resin from further combustion.

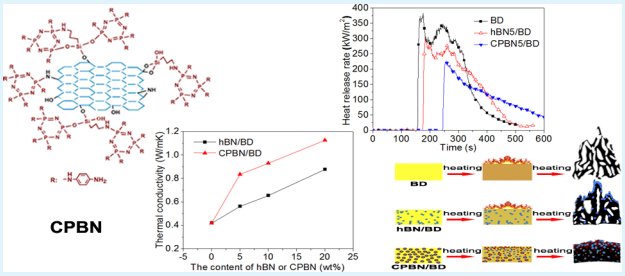

KEYWORDS: *hybridized fillers, hexagonal boron nitride, composites, thermal conductivity, flame retardancy*

1. INTRODUCTION

As functional materials, flame retarding polymers have been increasingly required by numerous industries from cutting-edges fields (such as aerospace, electric information, new energy, insulating, etc.)[1−3] to daily life related general fields (including decorates, construction, textile, and so on).[4,5] However, almost all polymers do not have good flame retardancy, and lots of researches have concluded that adding flame retardants into polymers is an effective way to prepare flame retarding polymers,[6,7] so the progress of flame retarding polymers greatly depends on the development of high performance flame retardants.

The concept of "high performance flame retardants" has been continuously updated to meet more and higher requirements of rapid development of industries, the main features are environment-friendly, high efficient and multifunctional. Note that high thermal resistance and thermal conductivity also become representative features of high performance flame retardants for IT and new energy fields;[8] however, few literature focused on this subject. One possible reason is that high thermal conductivity seems to be not beneficial to get high flame retardancy because the external heat may pass into the interior quickly, that is, it is not easy to prepare a material with simultaneously high thermal resistance and thermal conductivity. Another fact is that to obtain good flame retardancy or high thermal conductivity, different functional fillers have been used. Specifically, as organic materials generally do not have high thermal conductivity, so inorganic materials with high thermal conductivity have been often used to get high thermal conductivity. On the other hand, compared with organic flame retardants, inorganic flame retardants are environment-friendly, but their loadings are usually large, and some of them are even higher than 40 wt % to get good flame retardancy.[9−11] Therefore, to develop flame retardants with high thermal conductivity, inorganic/organic hybrids may be the right candidates.

In the past decade, many works focused on organic/inorganic hybrids because they have great possibility to inherit the merits and overcome the disadvantages of both organic and inorganic materials.[12−14] Up-to-date, only several hybrids were prepared to act as flame retardants; however, these hybrids did not have high thermal conductivity. Therefore, it is of great interest to make progress on this issue.

Hexagonal boron nitride (hBN) is known to be a layered material with super high thermal conductivity (200 W/mK),[15] which is one of the highest values owned by inorganic fillers. Besides, hBN also has other outstanding performances including good dimensional and thermal stability, desirable

Received: April 22, 2014
Accepted: August 20, 2014
Published: August 20, 2014

chemical and antioxidant ability.[15] Note that these performances are even better than graphenes,[15,16] however, unfortunately, the corresponding researches on hBN and related materials are very limited. One possible reason is that the content of active groups on the surface of hBN is so small that it is difficult to be functionalized. Up-to-date, only several research groups added hBN into epoxy resin,[17] polyimide,[18] or bismaleimide resin,[19] and found that the related composites have increased thermal stability or thermal conductivity compared with original resins. For example, after 2 wt % silane modified hBN was embodied into polyimide, the initial thermal degradation temperature (T_{di}, the temperature at which the weight loss is 5 wt %) increased about 15 °C;[18] while with the addition of 5 wt % hBN into bismaleimide resin, the T_{di} does not obvious change, but the thermal conductivity increases from 0.4 to 0.55 W/mK.[19]

Cyclophosphazene and derivatives are known to be effective flame retardants.[20] Kumar's[21,22] and Allcock's[23] groups studied polyimide and epoxy resin with cyclophosphazene, and found that the char yields at 700−800 °C of these polymers were as high as 80 wt %; moreover, when these polymers were used as matrices to prepare graphite fiber reinforced composites, the resultant composites could not burn even in a pure oxygen atmosphere.

This Research Article gives the first report on design and synthesis of new hybridized fillers with multifunctions, cyclophosphazene hybridized hBN (CPBN), which can be used as both flame retardant and thermal conductor. Considering the importance and great potential of applications,[24,25] *o*,*o*′-diallylbisphenol A (DBA) modified bismaleimide (BD) resin was chosen for evaluating the functional effects of CPBN. A series of CPBN/BD composites with different loadings of CPBN were prepared, moreover, the structure and properties of CPBN/BD composites were systematically investigated. Some interesting phenomena were founded, and the origin behind was studied.

2. EXPERIMENTAL SECTION

2.1. Materials. hBN with a purity of 99.3% was purchased from Zibo Jonye Ceramic Technologies Co., Ltd. (China), of which the average particle size was about 3 μm. 4,4′-Bismaleimidodiphenylmethane (BDM) was obtained from Northwestern Chemical Engineering Institute (China), DBA was provided by Soochow University (China), hexachlorocyclotriphosphazene (HCCP) with a purity of above 99% was purchased from Zibo Lanyin Chemical Co., Ltd. (China). *p*-Phenylenediamine (PDA) and triethylamine were obtained from Beijing Chemical Works (China). γ-Aminopropyl triethoxysilane (APTS) was bought from Zhangjiagang Guotai Huarong New Chemical Materials Co., Ltd. (China). Other reagents were commercial products with analytical grades and used without further treatment.

2.2. Synthesis of Cyclotriphosphazenes/hBN Hybrid (CPBN). hBN (1 g) and APTS (1 wt %) were dispersed in toluene (50 mL) with an ultrasonical agitation under a nitrogen atmosphere to form a mixture. The mixture was then stirred at 110 °C for 10 h and washed with absolute ethanol for several times, followed by drying at 80 °C for 12 h. The resultant product was denoted as aBN. These aBN particles were dispersed in tetrahydrofuran (THF) (50 mL) via ultrasonication to get a homogeneous mixture. The mixture and triethylamine (10 mL) were put into a 500 mL four-necked flask in an ice-bath with stirring at 0 °C for 1.5 h. And then the HCCP (2.0 g)/THF(50 mL) solution was slowly dropped into the flask within 2 h with stirring, followed by maintaining at 65 °C for 8 h under a nitrogen atmosphere to obtain a crude product. After that the crude product was filtered, washed, and dried, successively, to get the intermediate product, coded as HBN. The obtained HBN and 50 mL THF were put into a 500 mL four-necked flask, into which triethylamine (8 mL) was poured with stirring within 0.5 h. PDA (1.3 g) dissolved in 50 mL of THF was dropped into the flask within 0.5 h, and the reaction was carried out for 8 h with stirring at 65 °C under a nitrogen atmosphere. After that the particles were quickly vacuum-filtered to completely remove free HCCP, which was then washed using THF and absolute ethanol for several times, and dried at 80 °C for 12 h, successively. The resultant product was CPBN.

2.3. Preparation of BD Resin, hBN/BD, and CPBN/BD Composites. Appropriate quantities of BDM and BDA (the molar ratio of BDM to DBA was set at 1:0.86) were put into a beaker with a mechanical stirrer and a thermometer, and then the beaker was heated to 130−135 °C and maintained within that temperature range with stirring until a clear and brown liquid was obtained. After that, hBN particles with appropriate quantity were added into the liquid, and maintained at that temperature with stirring for an additional 30 min to get a hBN/BD prepolymer. The hBN/BD prepolymer was poured into a preheated glass mold and degassed under vacuum at 130 °C for 30 min. After that, the mold was put into an oven for curing using the procedure of 150 °C/2 h + 180 °C/2 h + 200 °C/2 h + 220 °C/2 h, and followed by a postcuring at 230 °C for 4 h. The resultant composite was coded as hBN*x*/BD, where *x* represents the mass fraction of hBN particles in the composite, taking values of 5, 10, and 20. Composites made up of CPBN and BD were also prepared according to the same process above, except that hBN was replaced by CPBN, and the resultant composite was named as CPBN*y*/BD, where *y* represents the mass fraction of CPBN in the composite, taking values of 5, 10, and 20. BD prepolymer and cured resins were also prepared following above procedure for hBN/BD composites except that no hBN was added.

Fourier Transform Infrared (FTIR) Spectra. Each sample was pressed into a pellet with KBr, which was then put into a Prostar LC240 infrared spectrometer (Agilent Technologies, Palo Alto, USA) for getting the FTIR spectrum between 400 and 4000 cm^{-1} at a resolution of 2 cm^{-1}.

Fluorescence Emission Spectra. The fluorescence emission spectra were measured using a QM/TM/IM steady-state and time-resolved fluorescence spectrofluorometer (PTI Ltd., USA) under an excitation at 291 nm.

X-ray Diffraction (XRD) Analyses. A MERCURY charge-coupled device X-ray diffractometer (Rigaku Tokyo, Japan) with Cuka radiation (λ = 0.154056) was used to record the XRD patterns. The 2θ angle ranged from 10° to 80°, and the scanning rate was 2 deg/min.

Scanning Electron Microscope (SEM). The morphologies of composites were observed by SEM (Hitachi S-4700, Tokyo, Japan) equipped with an energy dispersive spectrometry (EDS) attachment. Each sample was dried at 100 °C for 6 h before tests and then sprayed with a thin layer (about 10 nm) of gold.

Aberration-Corrected High-Angle Annular Dark-Field SEM Microscope (HAADF-STEM). A FEI TechaiG220 transmission electron microscope (TEM, USA) coupled with an EDS attachment operating at an acceleration voltage of 200 kV was employed to observe the STEM images of a sample and get various elemental mappings.

X-ray Photoelectron Spectroscopy (XPS). XPS spectra were recorded employing a Shimadzu-KRATOS Analytical-Axis ULTRA-DLD spectrometer (Manchester, U.K.) with monochromatized Al Kα X-ray source ($h\nu$ = 1486.71 eV) and a pressure in the analysis chamber of 10^{-9} Torr.

Thermogravimetric Analysis (TGA). A TGA SDTQ600 (TA Instruments, USA) was used to conduct TGA from 25 to 800 °C with a flowing rate of 100 mL/min and a heating rate of 10 °C/min in an air atmosphere.

Thermal Conductivity. Thermal conductivity at 20 °C was measured on a DRP-II thermal conductivity tester (Xiangtan Apparatus & Instruments, Xiangtan, China) using a steady-state method, and the upper copper plate was heated to 60 °C. The dimensions of each sample were Φ (70 ± 0.02) mm × (3 ± 0.02) mm. Three specimens were tested for each formulation, and the data reported herein are the averages of triplicate measurements.

Limited Oxygen Index (OI). OI values were measured with a Stanton Redcraft flame meter (London, U.K.) according to ASTM D 2863/77. The dimensions of each sample were (130 ± 0.02) mm × (6.5 ± 0.02) mm × (3 ± 0.02) mm. Three samples were tested for each composite, the values were reproducible within 0.5%, and the average value was used as the final result.

Cone Calorimeter (CONE) Testing. CONE tests were performed on an FTT device (UK) according to ISO 5660 with an incident flux of 35 kW/m^2. For each resin (composite), three specimens were tested. Each sample was put into an aluminum boat (tray), which was then put into the specimen holder in the horizontal orientation for testing. Typical results from CONE tests were reproducible to within about ±10%. The dimensions of each sample were (100 ± 0.02) mm × (100 ± 0.02) mm × (3 ± 0.02) mm.

Thermogravimetric Analysis Infrared (TG-IR). TG-IR spectra were recorded using a thermogravimetric analyzer (TGA F1, Netzsch, Germany) that was interfaced to a FTIR spectrophotometer (TENSOR 27, Bruker, Germany). Ten milligrams of a sample was put in an alumina crucible and heated from 40 to 800 °C with a heating rate of 10 °C/min under a nitrogen atmosphere, and the flowing rate was 45 mL/min.

3. RESULTS AND DISCUSSION

3.1. Synthesis and Characterization of CPBN. The route for synthesizing CPBN is illustrated in Figure 1, which contains

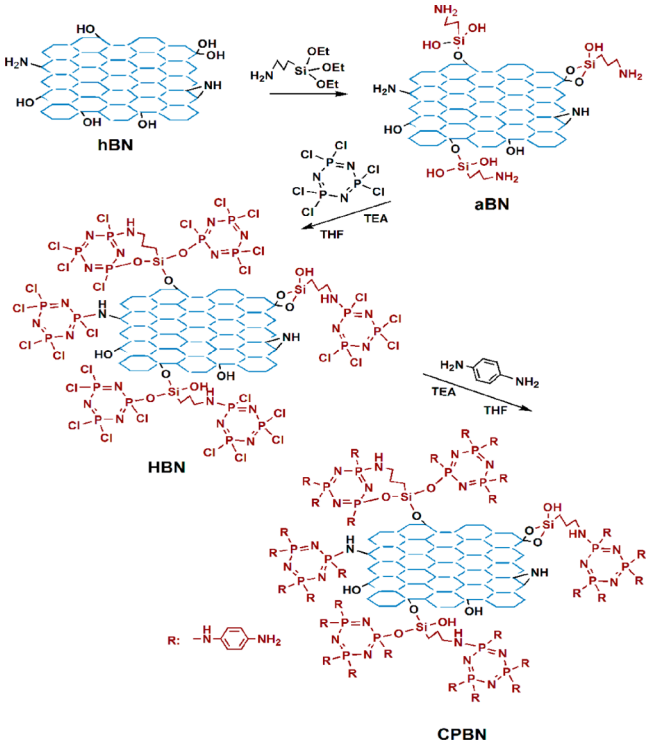

Figure 1. Synthesis of CPBN.

three steps. They are the introducing silane on the surface of hBN, the coating formation through the reaction between P−Cl groups and the amine or −OH groups, and the grafting of PDA through P−Cl and amine groups of PDA.

CPBN is a hybridized hBN, the most obvious difference between CPBN and hBN is their colors as shown in Figure 2A. Besides, hBN and HBN do not show any fluorescence effect, but CPBN exhibits a blue light fluorescence effect (Figure 2B) because of the electron transfer between the phenyl and amine groups of PDA,[26,27] and the chromaticity coordinates are x = 0.2059, y = 0.1911. These phenomena primarily suggest the success of synthesizing CPBN.

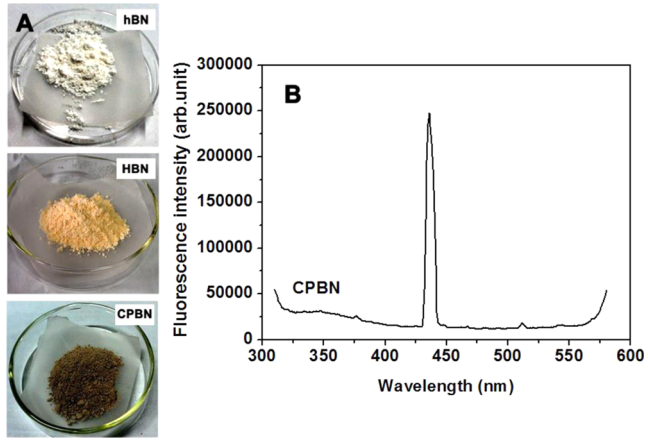

Figure 2. Digital photos of original and modified hBN powders (A); the fluorescence spectrum (B) of CPBN dispersed in ethanol (30 μg/mL).

Figure 3 shows the FTIR spectra of hBN and CPBN. Compared with the spectrum of hBN, that of CPBN shows

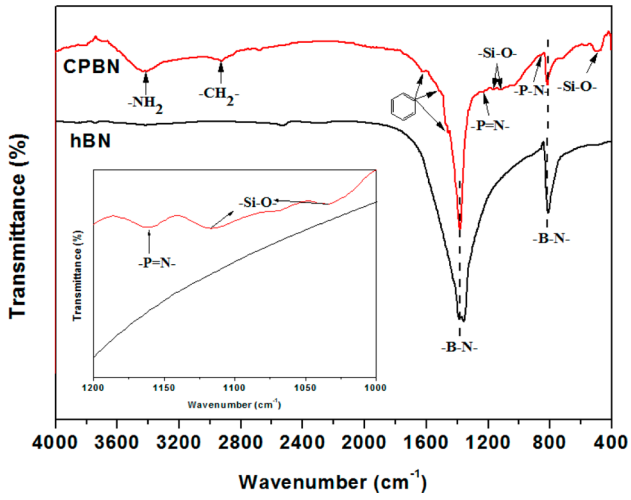

Figure 3. FTIR spectra of hBN and CPBN.

some new peaks, including the stretching vibrations of N−H (3408 cm^{-1}),[28] C−H (2925 cm^{-1}),[28,29] −Si−O− (1119, 1032, and 472 cm^{-1}),[29] phenyl ring (1620, 1509, and 1453 cm^{-1}),[28,29] −P═N− (at 1209 cm^{-1}), and −P−N− (842 cm^{-1}),[30] suggesting that CPBN contains the molecular features of APTES, HCCP, and PDA. Importantly, the absorption peak (601 cm^{-1}) assigning to the P−Cl group[31] of HCCP is hardly to be observed in the spectrum of CPBN, indicating the occurrence of grafting HCCP and PDA onto hBN.

From TG analyses (see Figure S1 in the Supporting Information), the composition of the coating on the hBN was calculated to be 8.80 wt %.

XRD is known to be a useful technique to give the composition, molecular structure and configuration information on inorganic materials.[28] Figure 4 shows the XRD patterns of samples during different stages for synthesizing CPBN. All samples have similar XRD patterns, and each pattern shows two strong diffraction peaks centered at 2θ = 26.7° and 41.7°, corresponding to (002) and (100) diffractions, respectively.[29]

dx.doi.org/10.1021/am502364k | ACS Appl. Mater. Interfaces 2014, 6, 14931−14944

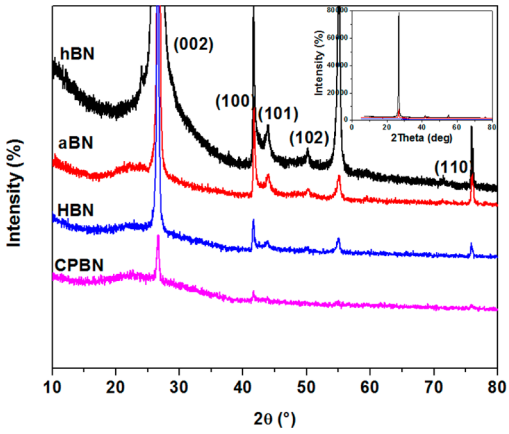

Figure 4. XRD patterns of hBN, aBN, HBN, and CPBN.

Furthermore, no new peak appears, so no new phase is formed during the synthesis of CPBN. Notably, the positions of these peaks do not change, but the pattern of CPBN shows notably weakened peaks (or even absent reflection) in the range of 2θ = 40−50°, where the 100, 101, and 102 lines of bulk hBN are found[32] compared with the pattern of hBN, suggesting that CPBN and hBN have different order structures.[32] This is also supported by the observed changes in the interlayer distance (d_{002}) and the thickness along the c axis (L_c) (see Table S1 in the Supporting Information). Especially, the L_c value of CPBN is about 80% of that of hBN, suggesting that the exfoliation appears and thus the size of fillers reduces during the synthesis process of CPBN. This phenomenon is also confirmed by the loosened shape of CPBN compared with the compact form of hBN as shown in the SEM micrographs (Figure 5A and 5B).

Figure 5C−5E gives TEM images of hBN and CPBN particles. The hBN flakes are laminar and smooth (Figure 5C); while CPBN particles have rough surfaces (Figure 5D and 5E), moreover, each of which is surrounded by a gray layer (bright area) with a thickness of about 6 nm (Figure 5E). This is an interesting phenomenon.

hBN particles do not have uniform dimensions, so do CPBN particles, this is also proved by the TEM photos of different CPBN particles shown in Figure 5D−5F. To clearly characterize the element distribution of CPBN, another CPBN with large dimension was selected to record its STEM image (Figure 5F) and corresponding EDS spectra (Figure 5G). It can be seen that the distribution of Si element is not as dense as those of C, O, and P elements, this is expected because the content of Si element is relatively smaller than those of other elements. The appearance of these elements reflects that the surface of CPBN is covered by an organic coating containing P, O and Si elements. On the other hand, the line EDS elemental mappings of B and P for CPBN (Figure 6) show that the content of P element in the rages of CPBN is relatively larger than that in the middle part; in contrast, the distribution of B element exhibits different trend, reflecting that a layer containing P element is coated on the surface of CPBN.

XPS technique was used to detect the difference in the chemical structure between hBN and CPBN. As shown in Figure 7A, the wide-scan spectra of hBN and CPBN are alike; however, compared with the spectrum of hBN, that of CPBN shows a new peak (at 134 eV) corresponding to P 2p.[33,34] The N 1s core level spectra (Figure 7B, 7C) were recorded to study the concentration of nitrogen-based functional groups on hBN and CPBN, it can be seen that the N 1s spectrum of hBN can be divided into two separate peaks attributing to −N−B− and −N−C− (the C element was introduced during the production process of hBN, confirmed by the manufacturer and the research conducted by Jaewoo's group[35]), respectively. The two peaks also appear in the spectrum of CPBN, meanwhile, there are two additional peaks assigning to −N−H− (~400.7 eV)

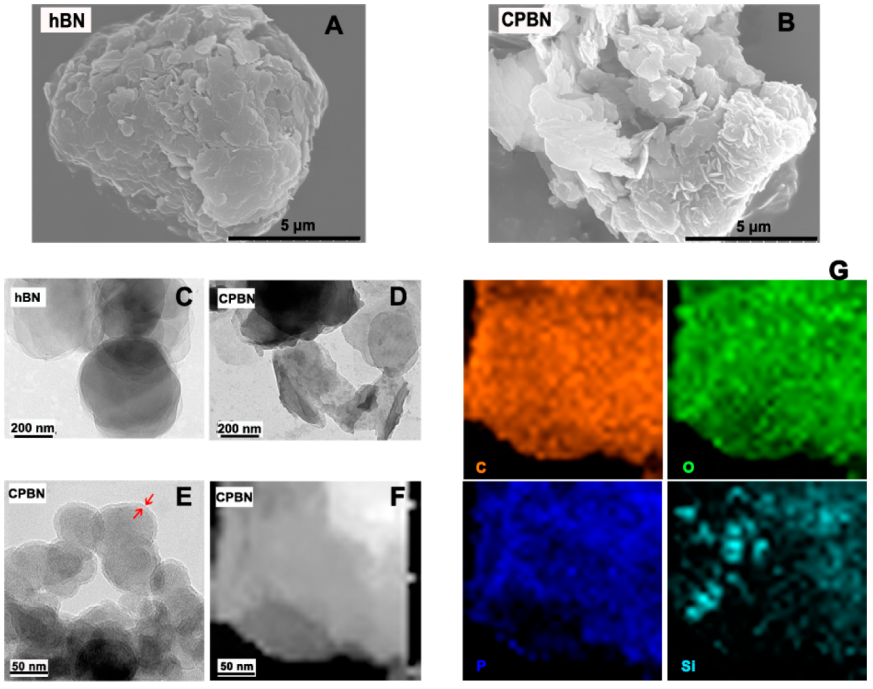

Figure 5. SEM (A, B) and TEM (C−E) images of hBN and CPBN; STEM image of CPBN (F) and XEDS elemental mappings (G) of C, O, P, and Si in (F).

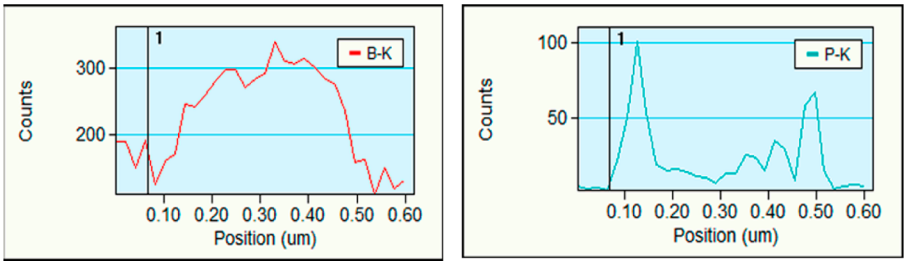

Figure 6. Line EDS elemental mappings of B and P for CPBN.

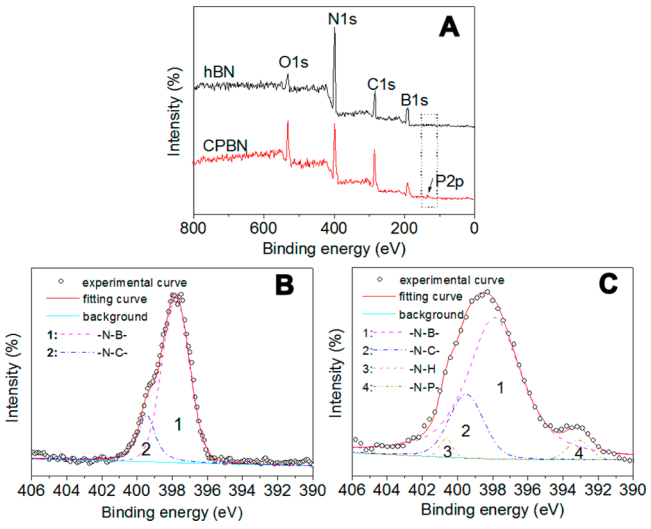

Figure 7. XPS spectra (A) and the N 1s core level spectra (B, C) of hBN and CPBN.

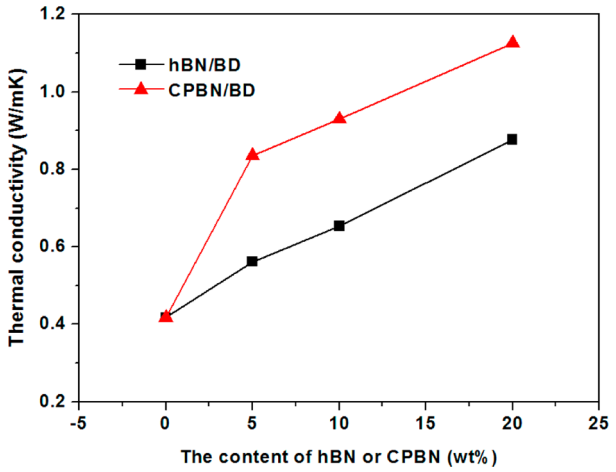

Figure 8. Thermal conductivities of BD resin, hBN/BD, and CPBN/BD composites.

and −N−P− groups (~393.7 eV),[36−38] demonstrating the occurrence of the hybridization of hBN.

On the basis of the above Results and Discussion, CPBN is a hybrid, of which hBN is chemically coated by an organic/inorganic layer containing cyclotriphosphazene, amine, Si−O−, and −OH groups.

3.2. Thermal Conductivities of CPBN/BD Composites. The aim of this paper is developing a new kind of functional fillers that can endow the resin with both high thermal conductivity and flame retardancy, so it is necessary to evaluate the thermal conductivity of CPBN/BD composites. Figure 8 depicts the thermal conductivities of cured BD resin, hBN/BD, and CPBN/BD composites. All composites have much higher thermal conductivities than BD resin, and the larger the content of CPBD is, the higher the thermal conductivity is. On the other hand, the CPBN/BD composite has higher thermal conductivity than the hBN/BD composite with the same content of fillers; this result is attractive and seems to be unexpected because cyclophosphazene is a material with low thermal conductivity.[39−42] It is known that the thermal conductivity is theoretically proportional to the transferring velocity and the mean free path of the phonons,[43] so the factors that can improve the interaction between fillers and the resin matrix, as well as the dispersion of fillers are beneficial to improve the thermal conductivity of a composite.

As discussed above that compared with hBN, CPBN has three differences in structure, including more active groups that will react with BD resin, reduced dimension and loosened connection between layers, these differences provide possibility for resin to enter into the layers of CPBN and make layers easy to be exfoliated during curing process, and consequently, resulting in good dispersion of CPBN in BD resin. As shown in Figure 9, hBN particles have serious aggregation in BD resin (Figure 9A1 and 9B1, 9A2, and 9B2); while CPBN particles have good dispersion, almost no obvious aggregation of white points is observed in the B mappings (Figure 9A3 and 9B3; 9A4 and 9B4). Therefore, it is reasonable to observe the results shown in Figure 8.

3.3. Flame Retardancy of CPBN/BD Composites. OI and CONE tests are two typical techniques to evaluate the flame retardancy and simulate the real fire of a material in a lab scale.[20] All composites have higher OI values than BD resin, and the OI value increases as the content of fillers increases (Figure 10), indicating that both CPBN and hBN have flame retarding effect. While, interestingly, the CPBN/BD composite has a significantly higher OI value than the hBN/BD composite with the same content of fillers, demonstrating that CPBN has a bigger flame retarding effect.

Table 1 summarizes typical CONE data of BD resin, hBN/BD, and CPBN/BD composites. CPBN/BD composites have much longer time to ignition (TTI) than BD resin and hBN/BD composites. This result is very attractive and meaningful because TTI represents the degree of difficulty in igniting a material.[44] The additions of many flame retardants tend to get reduced TTI values. For example, Cloisite 30B, a commercial organic-modified clay (montmorillonite), is known to be a good flame retardant for ethylene-vinyl acetate copolymer,[45,46] but it reduced TTI from 91 to 80 s.[47] When nano-oxides (Al_2O_3 and TiO_2)/ammonium polyphosphate was used as the flame retardant for poly(methyl methacrylate), the TTI value obviously decreased.[48] In fact, the biggest disadvantage of phosphate-containing flame retardants is that their addition

dx.doi.org/10.1021/am502364k | ACS Appl. Mater. Interfaces 2014, 6, 14931−14944

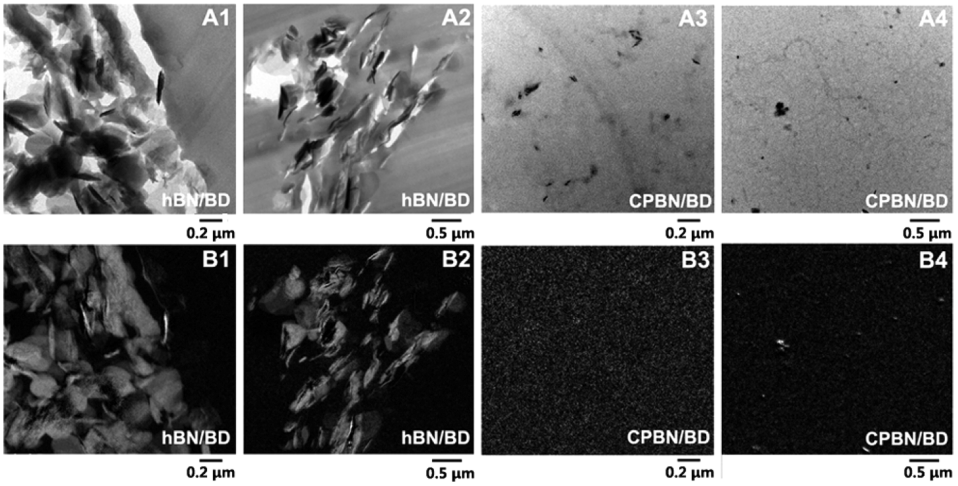

Figure 9. TEM micrographs (A1, A2, A3, A4) and B mappings (B1, B2, B3, B4) of two hBN5/BD and two CPBN5/BD composites.

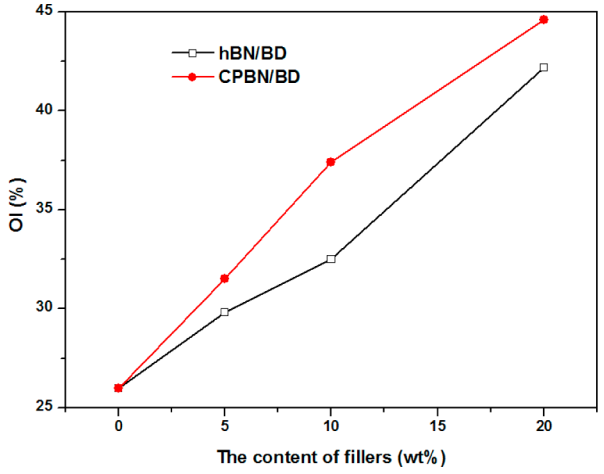

Figure 10. OI values of hBN/BD and CPBN/BD composites.

Table 1. Typical Parameters from CONE Tests for BD Resin, hBN/BD, and CPBN/BD Composites

	BD	hBN5/BD	hBN10/BD	CPBN5/BD	CPBN10/BD
TTI (s)	154	171	177	242	250
FPI ($s \cdot m^2/kW$)	0.40	0.57	0.62	1.07	1.21
FGI ($kW/(m^2 \cdot K)$)	2.17	1.65	1.51	0.88	0.80
PHRR (kW/m^2)	383	302	285	226	207
AHRR (kW/m^2)	175	141	100	78	77
THR (mJ/m^2)	62	55	46	55	44
MLR (g/s)	0.07	0.06	0.04	0.03	0.03
TSR (m^2/m^2)	2279	2160	1709	1037	936
TSP (m^2)	20	19	15	9	8
SEA (m/kg)	722	827	800	483	436
EHC (mJ/kg)	22	21	22	23	23

usually decreases the TTI value.[49] Therefore, CPBN does not exhibit the shortcoming of these flame retardants, instead, which shows super advantage in increasing TTI. This is attributed to the unique structure of CPBN as discussed later.

Besides TTI, fire performance index (FPI) and fire growth index (FGI) are two important parameters for evaluating the fire hazard of a material. Table 1 shows that the FPI values of hBN/BD and CPBN/BD composites are almost 1.4 and 2.7 times higher than that of BD resin, respectively, meaning that CPBN has a greater ability to increase the time to flashover or the available time for escaping in a full-scale fire situation.[50] In addition, the FGI values of hBN5/BD and CPBN5/BD composites are only about 76% and 40% of that of BD resin, respectively, meaning that a small addition of hBN or CPBN can effectively reduce the risk of catching fire and the combustion intensity of the resin. This is also supported by the overlay plots of heat release rate (HRR) versus time for BD resin, hBN5/BD, and CPBN5/BD composites (Figure 11).

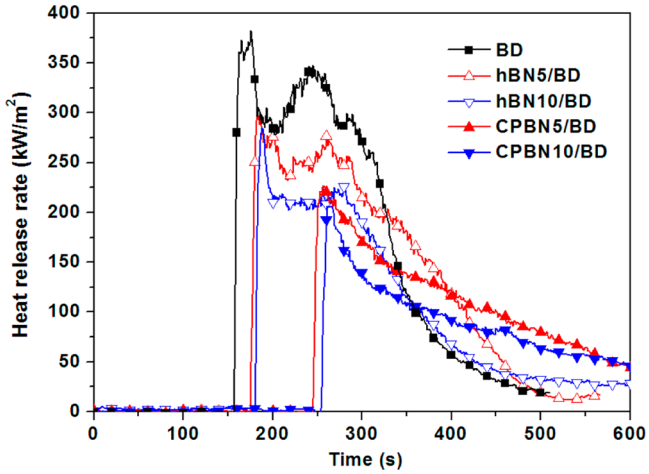

Figure 11. Overlay plots of dependence of HRR on time for BD resin, hBN/BD, and CPBN/BD composites.

As shown in Figure 11, the plot of cured BD resin contains a sharp peak as well as a broad and asymmetrical peak, indicating that the initially formed char is not strong enough to retard the continuous combustion. The curves of hBN/BD composites have similar shapes as that of the BD resin, but the former is much narrower and smaller than the latter. Interestingly, the curves of the CPBN/BD composites have obviously different shapes from others, demonstrating that the CPBN/BD composite has different flaming behavior.

For many materials, the effective heat of combustion (EHC) is constant for the whole burning of a specimen in the cone calorimeter, and a larger mass loss generally leads to higher HRR and poorer flame retardancy,[49,51] so the origin behind

these attractive results may be revealed through considering the integrated varieties of EHC and mass loss rate (MLR). Although all samples have almost equal EHC values (Table 1), they have obviously different dependence of the normalized mass loss on the time during the whole combustion process as shown in Figure 12. After ignition, BD resin quickly loses its

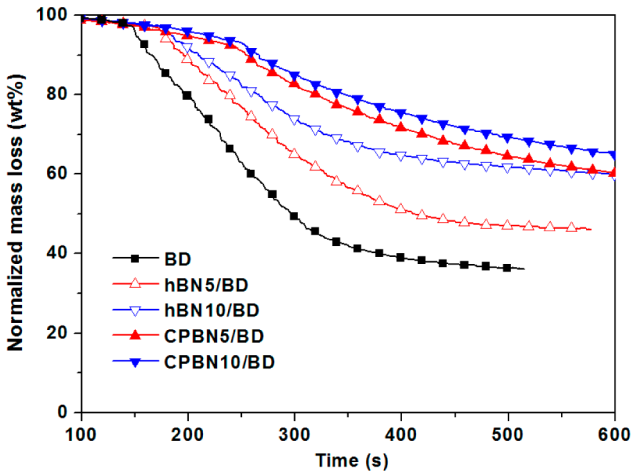

Figure 12. Overlay plots of dependence of normalized mass loss on time for BD resin, hBN/BD, and CPBN/BD composites.

weight, while the two kinds of composites, especially CPBN/BD composites, have much slower MLR values (Table 1), so the condensed phase flame retarding plays an important role in hBN/BD and CPBN/BD composites, which will be intensively discussed later.

Figure 13 shows the overlay curves of smoke produce rate (SPR)−time for resins and composites. Compared with the

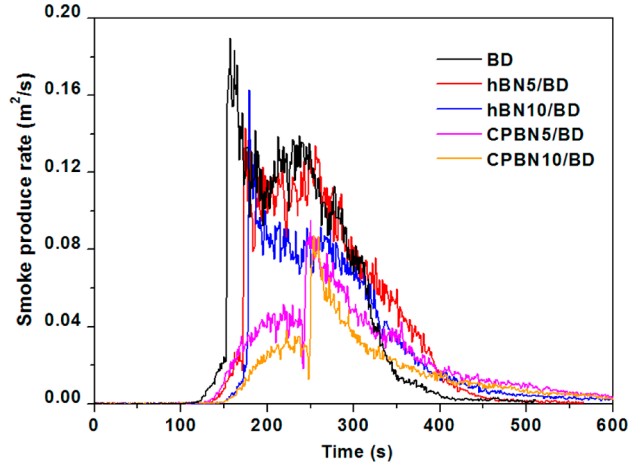

Figure 13. Overlay plots of dependence of SPR on time for BD resin, hBN/BD, and CPBN/BD composites.

peaks of BD resin, those of hBN/BD composites have similar shapes but weaker intensities; while CPBN/BD composites not only have the lowest SPR values among all samples, but also have obviously different shapes from others. With the addition of 5 and 10 wt % CPBN, the total smoke release (TSR) and total smoke production (TSP) are only 40−45% of that of BD resin, clearly demonstrating that CPBN/BD composites have high smoke suppression. This statement is further supported by the similar trend in specific extinction area (SEA) that reflects the smoke-producing ability of materials.[49]

The SPR curves of CPBN/BD composites can be divided into three parts, the first step is considered as an alarm of fire, including the appearance of smoke and the lasting period (100 s) before ignition; the time of this step is much shorter than the TTI value, meaning that the difficulty of the ignition is decreased with the addition of CPBN. The second step of the SPR curves is the rapid decrease to 0.04 m^2/s (about half of the peak value) of SPR after ignition, while the third step is the gradual decrease until the appearance of the flame out. This phenomenon is attributed to the unique structure of CPBN. Specifically, phosphate-containing component decomposes to produce phosphorus−oxygen acid (including some polymers), the composite with the phosphate-containing component will form a compact char layer that prevents the further combustion and heat transferring, leading to greatly reduced smoke releasing amount and thus improved flame retardancy.[49,52]

Note that the char of the CPBN5/BD composite after the CONE test is completely different from those of both BD resin and hBN5/BD composite (Figure 14). Specifically, both BD

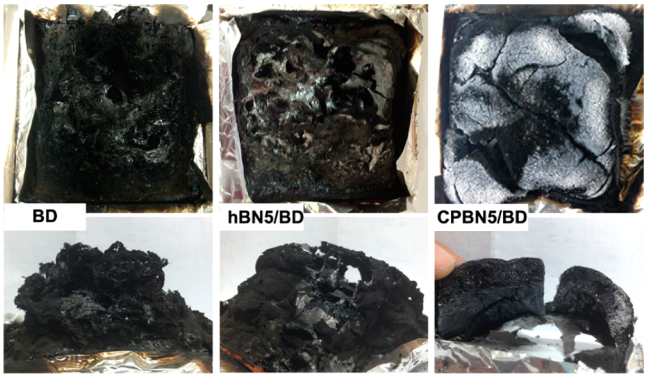

Figure 14. Digital photos of the chars of BD resin, hBN5/BD, and CPBN5/BD composites after CONE tests.

resin and hBN5/BD composite will greatly swell during combustion, and the maximum heights of the resultant chars are about 4 times of that of the CPBN5/BD char. Moreover, the BD and hBN5/BD chars are so thin and loose that they are easy to collapse, so the chars have irregular shapes; while the CPBN5/BD char is thick and relatively smooth with some broken crevices. On the other hand, some white substances are observed on the surfaces of the hBN5/BD and CPBN5/BD chars. Obviously, these differences originate from the difference in the structures of these cross-linked networks, the detail and intensive analyses and discussions are provided in the following part.

3.4. Flame Retarding Mechanism. Thermal stability, decomposition rate, production rate of char and char yield during the degradation process are three key factors to the flame retardancy of a polymer,[49,53] on which the rich knowledge can be obtained from the study on the thermodegradation kinetics, although less work was reported in the literature on the flame retarding polymers.

Figure 15 shows TG and DTG curves of BD resin, hBN5/BD and CPBN5/BD composites at different heating rates in an air atmosphere. The thermal decomposition of either original or modified BD resin contains two distinct stages divided by two DTG peaks, but these resins have different thermal

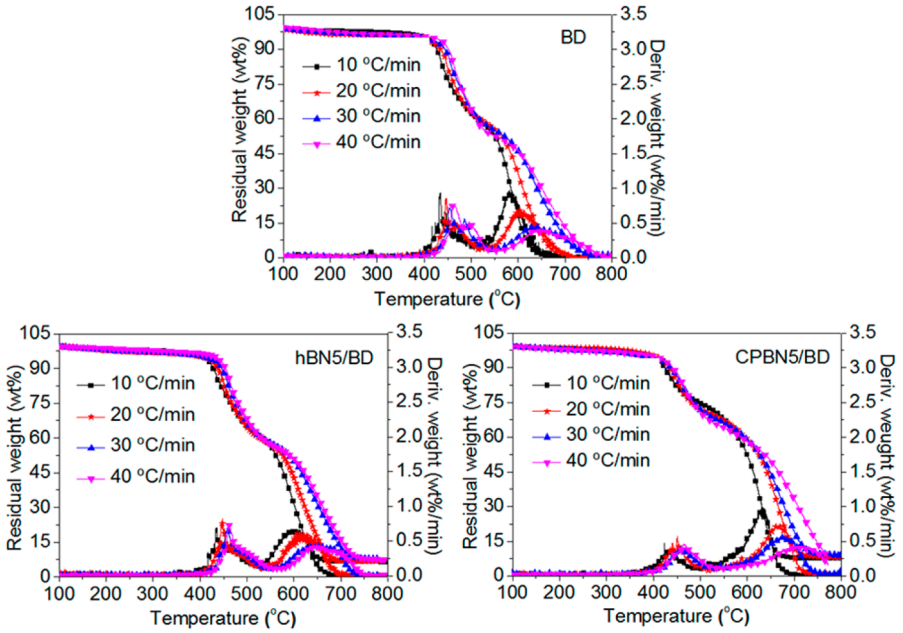

Figure 15. TG and DTG curves of BD resin, hBN5/BD, and CPBN5/BD composites in an air atmosphere.

Table 2. Activation Energies of Thermodegradation under an Air Atmosphere for Cured BD Resin, hBN5/BD, and CPBN5/BD Composites

	1st step					2nd step		
sample	Ea_1 (kJ/mol)	n_1	ln A_1	R_1	Ea_2 (kJ/mol)	n_2	ln A_2	R_2
BD	190	2.3	24.8	0.9902	123	1.3	8.91	0.9813
hBN5/BD	211	3.1	28.2	0.9943	138	1.5	10.7	0.9965
CPBN5/BD	224	4.2	30.3	0.9982	143	1.7	10.5	0.9967

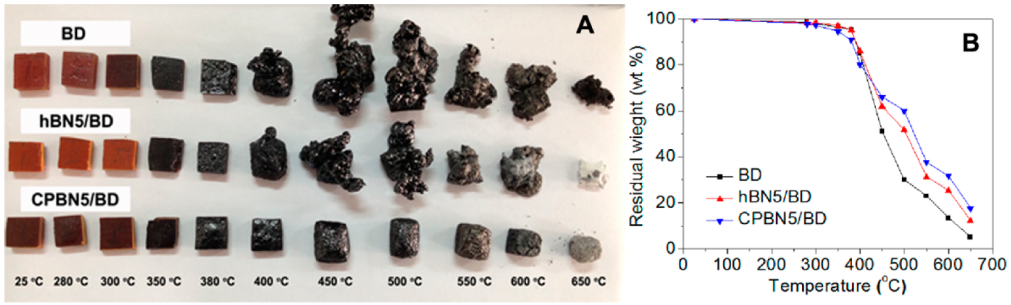

Figure 16. Digital photos (A) and residual weights (B) of BD resin, hBN5/BD, and CPBN5/BD composites after being maintained at different temperature for 15 min in a muffle furnace.

stabilities reflected by the T_{di} value.[54] As the CPBN5/BD composite has higher T_{di} than the hBN5/BD composite, so the former has better thermal-oxidative stability than the latter. In addition, the BD resin almost completely degrades at 650 °C, whereas hBN5/BD and CPBN5/BD composites have residual weights even at 800 °C, further indicating that the addition of either hBN or CPBN to BD resin can improve its thermal-oxidative stability at high temperature, and the CPBN5/BD composite has higher thermal-oxidative stability than the hBN5/BD composite.

According to the theory of nonisothermal kinetics and Arrhenius equation,[55,56] the thermal decomposition kinetics of resins and composites were calculated, the corresponding parameters such as active energy (Ea_1, Ea_1), reaction order (n_1, n_2), and pre-exponential factor (A_1, A_2) are summarized in Table 2. The composites (especially CPBN5/BD) have higher Ea_1 and Ea_2 values than the BD resin, meaning that the composites are more difficult to be degraded than the resin, while CPBN has a bigger ability to retard the degradation. On the other hand, CPBN5/BD composite has much bigger n_1 value and slightly bigger n_2 value than BD resin and hBN5/BD composite, so the whole degradation process of CPBN5/BD composite has a bigger dependence on the concentration of oxygen, this result coincides with the increased OI (Figure 10) and TTI (Table 1) values.

To intensively study the morphology change during heating, the photos of BD resin, hBN5/BD, and CPBN5/BD composites that had maintained at a preset temperature for 15 min in a muffle furnace were taken. As shown in Figure 16, both BD resin and hBN5/BD composite cannot retain their shapes after being maintained at the temperatures higher than 400 °C, especially, their volumes significantly expand at 500 °C,

dx.doi.org/10.1021/am502364k | ACS Appl. Mater. Interfaces 2014, 6, 14931−14944

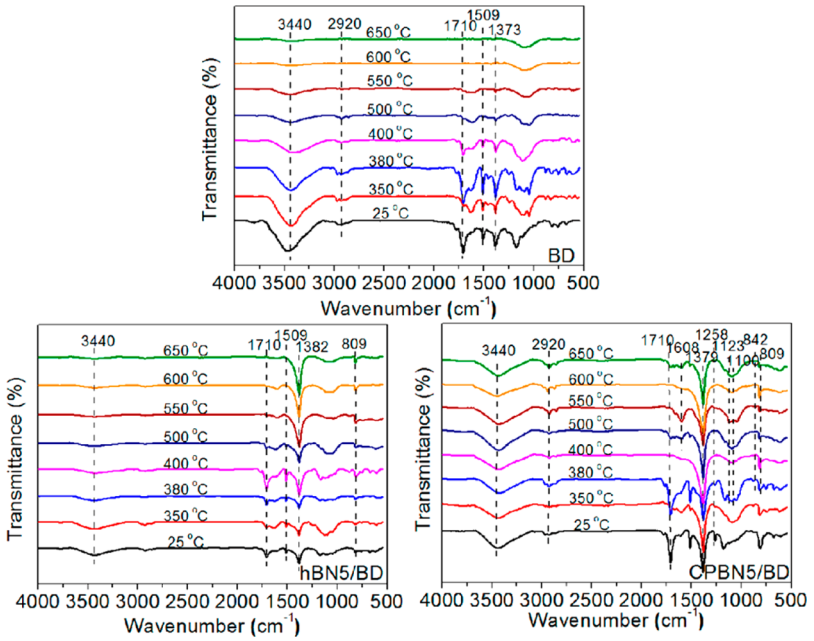

Figure 17. FTIR spectra of the chars of BD resin, hBN5/BD, and CPBN5/BD composites after maintained at different temperature for 15 min in a muffle furnace.

Table 3. Elemental Compositions of the Residues for BD Resin, hBN5/BD, and CPBN5/BD Composites after Maintained at Different Temperatures

			elemental composition (wt %)					elemental ratio (%)
residue			C	N	O	P	Si	C/O
BD	25 °C	external	73.81	9.48	16.71	0	0	4.42
		internal	73.07	7.96	18.96	0	0	3.85
	350 °C	external	70.68	9.50	19.81	0	0	3.57
		internal	73.01	7.39	19.59	0	0	3.73
	550 °C	external	78.63	13.15	8.22	0	0	9.57
		internal	78.34	8.18	13.48	0	0	5.81
	650 °C	external	79.41	11.96	8.63	0	0	9.20
		internal	81.18	12.72	6.10	0	0	13.31
hBN5/BD	25 °C	external	66.46	15.24	18.31	0	0	3.63
		internal	71.98	13.15	14.87	0	0	4.84
	350 °C	external	63.21	15.63	21.16	0	0	2.99
		internal	74.45	10.86	14.69	0	0	5.07
	550 °C	external	62.05	25.40	12.55	0	0	4.94
		internal	79.86	8.39	11.76	0	0	6.79
	650 °C	external	4.89	87.06	8.05	0	0	0.61
		internal	18.65	73.54	7.81	0	0	2.39
CPBN5/BD	25 °C	external	73.61	9.90	16.15	0.18	0.16	4.56
		internal	73.36	10.01	16.33	0.17	0.13	4.49
	350 °C	external	73.20	9.21	17.31	0.17	0.11	4.23
		internal	73.90	9.63	16.07	0.21	0.19	4.60
	550 °C	external	65.73	21.74	11.07	0.91	0.55	5.94
		internal	67.80	13.45	18.43	0.13	0.19	3.68
	650 °C	external	34.03	45.03	16.12	2.71	1.71	2.11
		internal	71.13	16.45	11.26	0.85	0.31	6.32

and then remarkably decrease as the temperature further increases. Note that, during the whole change process in the volume, the mass of BD resin rapidly decreases as the maintained temperature increases; moreover, when the sample is maintained at temperature higher than 550 °C, it becomes a "shell" made up of many holes, suggesting that the carbon produced during the decomposition does not form a compact layer, and thus the resin cannot be well protected. For the sample after stayed at 650 °C for 15 min, its residual mass is only 4.99 wt % of that of original resin (Figure 16B), and no peak attributing to organic groups can be observed in its FTIR spectrum (Figure 17).

The hBN5/BD composite shows a similar phenomenon; however, the volume of hBN5/BD composite is not as large as that of BD resin when the temperature is higher than 400 °C. And it is interesting to find that the surface of hBN5/BD char is

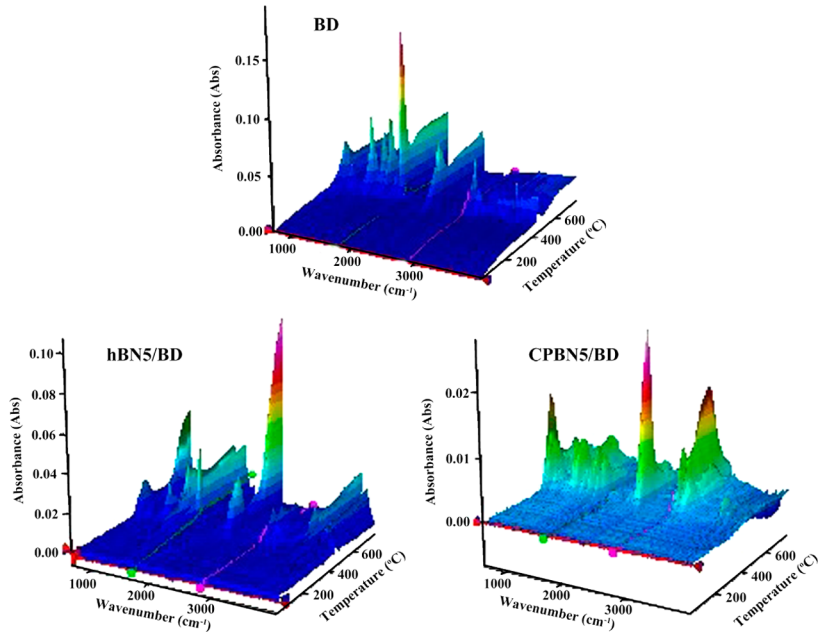

Figure 18. Three-dimensional FTIR spectra of the gaseous volatiles evolved during the combustion processes of BD resin, hBN5/BD, and CPBN5/BD composites in a N_2 atmosphere.

covered by a layer of white substance when the temperature is higher than 600 °C, and the phenomenon enhances as the temperature increases. The white substance is proved to be hBN due to the appearance of the vibration peak assigning to −B−N− bonds at 1382 and 809 cm^{-1}[57,58] in the FTIR spectra (Figure 17).

The CPBN5/BD char maintains a good dimensional stability and is very compact without any pore during the whole experiment; moreover, which has much larger residual masses at high temperature (>450 °C) than the BD and hBN5/BD residues, demonstrating that the addition of CPBN can endow the cross-linked network with very good dimensional and thermal stability. This statement is further confirmed by the appearance of the characteristic absorptions of organic bonds, including imide ring (3440 cm^{-1}) and DBA (2920, 1710, 1600 cm^{-1}),[59] in the FTIR spectrum of CPBN5/BD residue after being maintained at 650 °C (Figure 17); and the surface of CPBN5/BD char is also covered with a layer of hBN, proved by the vibration peak assigning to B−N− bonds at 1382 and 809 cm^{-1} shown in FTIR spectrum (Figure 17),[57,58] so the organic resin has been protected from a complete decomposition with the presence of CPBN.

Table 3 shows the elemental compositions of the residues for BD resin, hBN5/BD, and CPBN5/BD composites after maintained at different temperatures. During the whole process, the element concentrations of the external or internal part of BD char are substantially the same, indicating that the internal and external parts have similar combustion behavior, in other words, the char generated on the surface of BD resin during combustion can not effectively protect the inner resin from decomposition. When the temperature is higher than 550 °C, the relative C/O element ratio on the surface increases by almost 2 times, and the contents of C and N elements increase, suggesting that the groups containing O element have a significant degradation at this temperature. After heated at 650 °C, the internal element compositions are similar as the external compositions, but some organic compounds are still remained according to the content of N element.

For the hBN5/BD composite, its external and internal parts have different element distributions, indicating that hBN particles do not show a good dispersion in the composite at the room temperature. The content of the N element increases sharply when the sample is maintained at the temperature higher than 550 °C, while the C/O element ratio increases a little compared with the samples at low temperatures, suggesting that the organic composition begins to decompose but the organic groups still remains, meaning that hBN particles begin to aggregate on the surface of the sample. When the temperature is as high as 650 °C, the content of N element on the surface increases to 87%, while the C content is only 4.89%, indicating that almost only hBN left, and either the organic compounds or inorganic char has almost been decomposed; at this time, the N content of the interior is as high as 73.5%, but the C content is much higher than that on the surface, illustrating that hBN on the surface plays an effective role in protecting the organics from combustion.

With regard to CPBN5/BD composite, its element dispersions of the external and internal parts are similar, so CPBN particles exhibit an excellent distribution in the composite at 25 °C. After the sample was maintained at temperature higher than 550 °C, the C/O element ratio does not obviously change and is similar as that of hBN5/BD composite; while the contents of N, P, and Si elements increase by 1, 5, and 3 times, respectively, suggesting that the content of inorganic component increases; moreover, the increased contents of P and Si elements illustrate that the groups containing P or Si of CPBN in the composite have decomposed, and gathered on the surface of the sample by the joint action of heat and air flows. This phenomenon is enhanced for the sample maintained at 650 °C, and the contents of N and C elements on the surface of the sample are 45% and 34%, respectively; such high content of C element suggests that the char generated on the surface has high stability even at 650 °C. In the internal part, the content of C element is even higher than that of N element, indicating that there is considerable concentration of organic composition left without

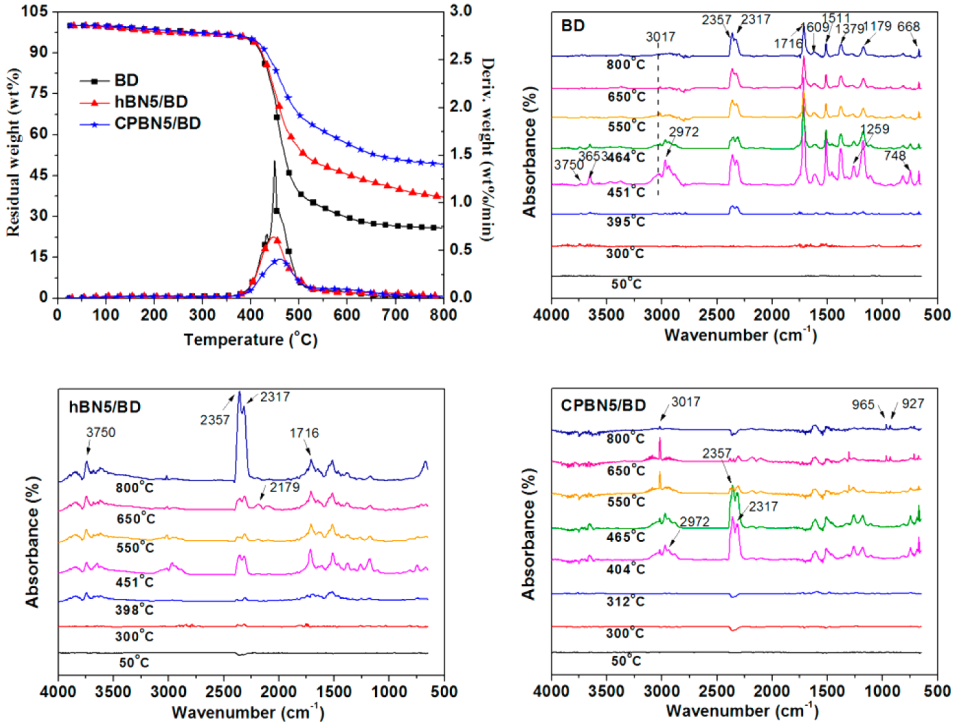

Figure 19. TG curves and FTIR spectra of volatilized products at typical temperatures during the thermal degradation for BD resin, hBN5/BD, and CPBN5/BD composite.

decomposition, that is to say that CPBN has outstanding protection role.

To obtain more understanding of the flame retarding mechanism, TG-IR spectra of pyrolysis products of BD resin, hBN5/BD and CPBN5/BD composites in a N_2 atmosphere were recorded. Figure 18 shows the three-dimensional FTIR spectra of gaseous volatiles evolved during the whole combustion processes of BD resin, hBN5/BD, and CPBN5/BD composites. As same parameters including the size, shape and weight of samples were used for tests, so the absorption intensity of peaks can be used to evaluate the relative amount of the pyrolysis products. It can be seen that the CPBN5/BD composite releases the fewest amount of products, while the BD resin has the most amount. This statement is also confirmed by the TG curve (Figure 19), and coincides with the flame retarding results discussed above.

Figure 19 gives the FTIR spectra of each sample at typical temperatures, including T_{di}, the temperature of the maximum degradation rate (T_{max}). For BD resin, a slight absorption peak assigning to carbonyl-containing compounds (1500−1700 cm^{-1})[59,60] is observed when the temperature reaches 300 °C; at T_{di} (395 °C), the peak for CO_2 (2300−2400 cm^{-1})[61,62] is clearly observed. These peaks are greatly enhanced and more peaks appear as the temperature increases, specifically, when the temperature increases to 451 °C (T_{max}), the peaks attributing to O−H bond (3750, 3653, and 1259 cm^{-1}, relating to H_2O generation),[63,64] aromatic compounds (1511, 1607, and 3017 cm^{-1}),[59,60] aliphatic components (2972, 1259, and 748 cm^{-1}),[59] and nitrogen compounds (1179 cm^{-1})[65] appear. The C−H peak (2800−3100 cm^{-1})[66] reaches the maximum values at 464 °C, and then disappear at 550 °C.

Compared with BD resin, hBN5/BD composite has similar T_{di} and T_{max} values but higher char yield at 800 °C (Y_c) that is even larger than the calculated value based on the "mixture role". The FTIR spectra at low temperature ($<T_{max}$) of hBN5/BD composite are alike as those of BD resin, while the spectra of hBN5/BD composite at temperature higher than T_{max} are different from those of BD resin. Specifically, the peaks over 2800−3100 cm^{-1} still exist, indicating that the pyrolysis products at high temperature still have rich compositions, that is, the decomposition of organic resin has been delayed because of the presence of hBN.

For the CPBN5/BD composite, its T_{di}, T_{max}, and Y_c at 800 °C are much higher than those of BD resin and hBN5/BD composite, clearly demonstrating that CPBN can effectively retard the decomposition of BD resin and has super ability of char formation. With regard to the FTIR spectra of pyrolysis products of the CPBN5/BD composite, they have some interesting differences compared with those of BD resin and hBN5/BD composite. First, no peak is observed until the temperature reaches 312 °C, at which only slight peak for carbonyl-containing components (1500−1800 cm^{-1}) is observed, this is in good agreement with the remarkably increased TTI value (Table 1). Second, when the temperature is higher than 550 °C, the peak from aromatic compounds (3017 cm^{-1}) becomes stronger, meanwhile two peaks representing C−N bond (965 and 927 cm^{-1})[63,67] appear, suggesting the degradation of the organic coating on CPBN. On the other hand, it is worthy to note that the typical peaks representing phosphorus-containing (P−N, P−O, P−C) bonds or silicon-containing bonds are not observed in the FTIR spectra of pyrolysis products of CPBN5/BD composite, clearly demonstrating that cyclotriphosphazene and Si-containing bonds remain in the residue, in other word, they play role in the condensed phase.

On the basis of the above analyses, it is reasonable to state that the BD resin, hBN/BD, and CPBN/BD composites have different combustion processes and flame retarding mechanisms. Figure 20 gives the schematic flame retarding mechanisms of these samples. In detail, the BD resin starts to

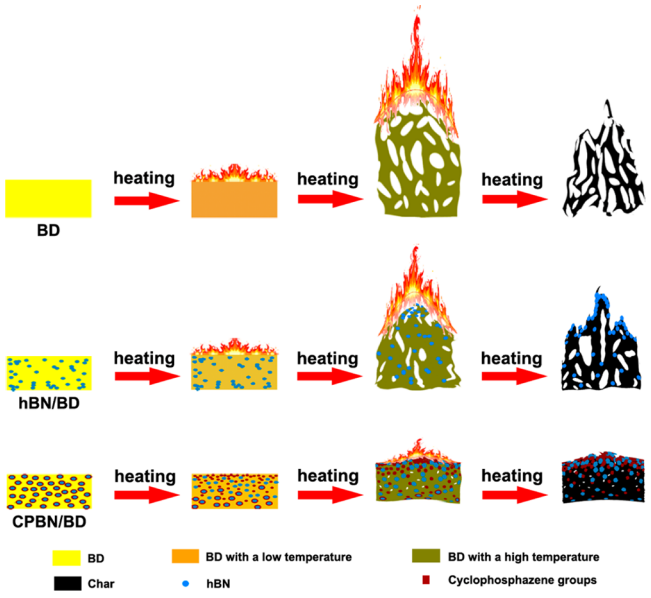

Figure 20. Schematic combustions of BD resin, hBN5/BD, and CPBN5/BD composites.

degrade when it is heated to a certain temperature, and the char on the surface does not have a sufficient protection.

In the hBN/BD composite, hBN particles do not have good dispersion in the resin, so hBN particles could not effectively protect the resin from combustion. After combustion, the organic parts on the surface decompose, and then the left hBN particles tend to gather with the aid of the flow of the gas, gradually forming a layer of hBN layer, which can retard the decomposition of the inner resin.

For the CPBN/BD composites, the CPBN particles have good dispersion in the resin owing to their good interaction with BD resin, this can effectively improve the thermal stability of the composite. Only when the heat is high enough, the resin begins to decompose with slow rate. While P–N and P–O bonds of CPBN are easily broken because their bond energies are relatively low,[67,68] the P flame retardants released from CPBN increase the ability of char formation, but do not play role in the gas-phase. Therefore, a dense and thermally stable char containing hBN is produced on the surface of the sample, which isolates the resin from oxygen and heat and thus protects the inner resin from decomposition.

4. CONCLUSIONS

CPBN is a new hybridized hBN. CPBN/BD composites with suitable loadings of CPBN particles have not only significantly improved flame retardancy, but also much higher thermal stability and thermal conductivity, demonstrating that CPBN has attractive multifunctional effects due to the unique structure of CPBN. Specifically, the fruit active groups on CPBN endow the good dispersion in BD resin, while the cyclotriphosphazene released from CPBN makes the composites prefer to form dense and thermally stable char containing hBN, leading to significantly improved flame retardancy.

■ ASSOCIATED CONTENT

Supporting Information

TG curves of hBN and CPBN and typical parameters from XRD patterns of hBN, aBN, HBN, and CPBN. These materials are available free of charge via the Internet at http://pubs.acs.org.

■ AUTHOR INFORMATION

Corresponding Authors

*Tel: +86 512 65880967. Fax: +86 512 65880089. E-mail: lgzheng@suda.edu.cn.

*Tel: +86 512 65880967. Fax: +86 512 65880089. E-mail: ajgu@suda.edu.cn.

Notes

The authors declare no competing financial interest.

■ ACKNOWLEDGMENTS

The authors thank Natural Science Foundation of China (21274104), and the Priority Academic Program Development of Jiangsu Higher Education Institutions (PAPD) for financially supporting this project.

■ REFERENCES

(1) Qian, L. J.; Ye, L. J.; Qiu, Y.; Qu, S. R. Thermal Degradation Behavior of the Compound Containing Phosphaphenanthrene and Phosphazene Groups and Its Flame Retardant Mechanism on Epoxy Resin. *Polymer* **2011**, *52*, 5486–5493.

(2) Ran, S. Y.; Guo, Z. H.; Chen, C.; Zhao, L. P.; Fang, Z. P. Carbon Nanotube Bridged Cerium Phenylphosphonate Hybrids, Fabrication, and Their Effects on the Thermal Stability and Flame Retardancy of the HDPE/BFR Composite. *J. Mater. Chem. A* **2014**, *2*, 2999–3007.

(3) Sun, J.; Wang, X. D.; Wu, D. Z. Novel Spirocyclic Phosphazene-Based Epoxy Resin for Halogen-Free Fire Resistance: Synthesis, Curing Behaviors, and Flammability Characteristics. *ACS Appl. Mater. Interfaces* **2012**, *4*, 4047–4061.

(4) Kim, Y. S.; Li, Y. C.; Pitts, W. M.; Werrel, M.; Davis, R. D. Rapid Growing Clay Coatings to Reduce the Fire Threat of Furniture. *ACS Appl. Mater. Interfaces* **2014**, *6*, 2146–2152.

(5) Zhang, X.; He, Q. L.; Gu, H. B.; Colorado, H. A.; Wei, S. Y.; Guo, Z. H. Flame-Retardant Electrical Conductive Nanopolymers Based on Bisphenol F Epoxy Resin Reinforced with Nano Polyanilines. *ACS Appl. Mater. Interfaces* **2013**, *5*, 898–910.

(6) Kang, N. J.; Wang, D. Y.; Kutlu, B.; Zhao, P. C.; Leuterita, A.; Wagenknecht, U.; Heinrich, G. A New Approach to Reducing the Flammability of Layered Double Hydroxide (LDH)-Based Polymer Composites: Preparation and Characterization of Dye Structure-Intercalated LDH and Its Effect on the Flammability of Polypropylene-Grafted Maleic Anhydride/d-LDH Composites. *ACS Appl. Mater. Interfaces* **2014**, *5*, 8991–8997.

(7) Zhao, B.; Chen, L.; Long, J. W.; Jian, R. K.; Wang, Y. Z. Synergistic Effect between Aluminum Hypophosphite and Alkyl-Substituted Phosphinate in Flame-Retarded Polyamide 6. *Ind. Eng. Chem. Res.* **2013**, *52*, 17162–17170.

(8) Cao, J. P.; Zhao, X. D.; Zhao, J.; Zha, J. W.; Hu, G. H.; Dang, Z. M. Improved Thermal Conductivity and Flame Retardancy in Polystyrene/Poly(vinylidene fluride) Blends by Controlling Selective Localization and Surface Modification of SiC Nanoparticles. *ACS Appl. Mater. Interfaces* **2014**, *5*, 6915–6924.

(9) Rothon, R. *The Emergence of Magnesium Hydroxide as a Fire Retardant Additive*, The Plastic and Rubber Institute Flame Retardants 1990 Conference; Elsevier: London, 1990.

(10) Dasari, A.; Yu, Z. Z.; Mai, Y. W.; Liu, S. l. Flame Retardancy of Highly Filled Polyamide 6/Clay Nanocomposites. *Nanotechnology* **2007**, *7*, 1–10.

(11) Haurie, L.; Fernández, A. I.; Velasco, J. I.; Chimenos, J. M.; Cuesta, J-M. L; Espiell, F. Synthetic Hydromagnesite as Flame Retardants. Evaluation of the Flame Behaviour in a polyethylene Matrix. *Polym. Degrad. Stab.* **2006**, *91*, 989–994.

(12) Zhang, M. C.; Gu, A. J.; Liang, G. Z.; Yuan, L. Preparation of High Thermal Conductive Aluminum Nitride-Cyanate Ester Nano-

composite Using a New Macromolecular Coupling Agent. *Polym. Adv. Technol.* **2012**, *23*, 1503−1510.
(13) Zeng, L.; Liang, G. Z.; Gu, A. J.; Yuan, L.; Zhuo, D. X.; Hu, J. T. High Performace Hybrids Based on a Novel Incompletely Condensed Polyhedral Oligomeric Silsesquioxane and Bismaleimide Resin with Improved Thermal and Dielectric Properties. *J. Mater. Sci.* **2012**, *47*, 2548−2558.
(14) Anbazhagan, S.; Alagar, M.; Gnanasundaram, P. Synthesis and Characterization of Characterization of Organic-Inorganic Hybrid Clay Filled and Bismaleimide-Siloxane Modified Epoxy Nanocomposites. *Int. J. Plast. Technol.* **2011**, *15*, 30−45.
(15) Golberg, D.; Bando, Y.; Huang, Y.; Terao, T.; Mitome, M.; Tang, C. C.; Zhi, C. Y. Boron Nitride Nanotubes and Nanosheets. *ACS Nano* **2010**, *4*, 2979−2993.
(16) Shi, Y. M.; Li, L.-J. Chemically Modified Graphene: Flame Retardant or Fuel for Combustion? *J. Mater. Chem.* **2011**, *21*, 3277−3279.
(17) Yu, J. H.; Huang, X. Y.; Wu, C.; Wu, X. F.; Wang, G. L.; Jiang, P. K. Interfacial Modification of Boron Nitride Nanoplatelets for Epoxy Composites with Improved Thermal Properties. *Polymer* **2012**, *53*, 471−480.
(18) Kizilkaya, C.; Mülazim, Y.; Kahraman, M. V.; Apohan Nilhan, Kayaman.; Güngör, A. Synthesis and Characterization of Polyimide/Hexagonal Boron Nitride Composite. *J. Appl. Polym. Sci.* **2012**, *124*, 706−712.
(19) Gao, Y. W.; Gu, A. J.; Jiao, Y. C.; Yang, Y. L.; Liang, G. Z.; Hu, J. T.; Yao, W.; Yuan, L. High-Performance Hexagonal Boron Nitride/Bismaleimide Composites with High Thermal Conductivity, Low Coefficient of Thermal Expansion, and Low Dielectric Loss. *Polym. Adv. Technol.* **2012**, *23*, 919−928.
(20) Lu, S.-Y.; Hamerton, I. Recent Developments in the Chemistry of Halogen-Free Flame Retardant Polymers. *Prog. Polym. Sci.* **2002**, *27*, 1661−1712.
(21) Kumar, D.; Gupta, A. D. Aromatic Cyclolinear Phosphazene Polyimides Based on a Novel Bis-Spiro-Substituted Cyclotriphosphazene Diamine. *Macromolecules* **1995**, *28*, 6323−6329.
(22) Kumar, D.; Fohlen, G. M.; Paker, J. A. The Curing of Epoxy Resins with Aminophenoxycyclotriphosphazenes. *J. Polym. Sci., Part A: Polym. Chem.* **1986**, *24*, 2415−2424.
(23) Allcock, H. R. Poly(Organophosphazenes)—Unusual New High Polymers. *Angew. Chem., Int. Ed. Engl.* **1977**, *16*, 147−156.
(24) Gu, A. J.; Liang, G. Z.; Liang, D.; Ni, M. Bismaleimide/Carbon Nanotube Hybrids for Potential Aerospace Application: I. Static and Dynamic Mechanical Properties. *Polym. Adv. Technol.* **2007**, *18*, 835−840.
(25) Peterson, A. M.; Jensen, R. E.; Palmese, G. R. Room-Temperature Healing of a Thermosetting Polymer Using the Diels−Alder Reaction. *ACS Appl. Mater. Interfaces* **2010**, *2*, 1141−1149.
(26) Wei, W.; Huang, X. B.; Chen, K. Y.; Tao, Y. M.; Tang, X. Z. Fluorescent Organic−Inorganic Hybrid Polyphosphazene Microspheres for the Trace Detection of Nitroaromatic Explosives. *RSC Adv.* **2012**, *2*, 3765−3771.
(27) Aslan, F.; Halci, O.; Arslan, M. Synthesis, Characterization and Fluorescence Phenomena of 1-Naphthoxy and 1-Naphthylamino Substituted-Cyclotriphosphazenes. *Heteroat. Chem.* **2008**, *19*, 158−162.
(28) Ye, J. H.; Liang, G. Z.; Gu, A. J.; Zhang, Z. Y.; Han, J. P.; Yuan, L. Novel Phosphorus-Containing Hyperbranched Polysiloxane and Its High Performance Flame Retardant Cyanate Ester Resins. *Polym. Degrad. Stab.* **2013**, *98*, 597−608.
(29) Zhang, X.; Zhong, Y.; Mao, Z. P. The Flame Retardancy and Thermal Stability Properties of Poly(Ethylene terephthalate)/Hexakis-(4-nitrophenoxy) Cyclotriphosphazene Systems. *Polym. Degrad. Stab.* **2012**, *97*, 1504−1510.
(30) Bao, C. L.; Guo, Y. Q.; Song, L.; Kan, Y. C.; Qian, X. D.; Hu, Y. In Situ Preparation of Functionalized Graphene Oxide-Epoxy Nanocomposites with Effective Reinforcements. *J. Mater. Chem.* **2011**, *21*, 13290−13298.
(31) Li, D.; Qin, Q.; Duan, X. C.; Yang, J. Q.; Guo, W.; Zheng, W. J. General One-Pot Template-Free Hydrothermal Method to Metal Oxide Hollow Spheres and Their Photocatalytic Activities and Lithium Storage Properties. *ACS Appl. Mater. Interfaces* **2013**, *5*, 9095−9100.
(32) Paine, R. T.; Narula, C. K. Synthetic Routes to Boron Nitride. *Chem. Rev.* **1990**, *90*, 73−91.
(33) Viornery, C.; Chevolot, Y.; Léonard, D.; Aronsson, B. O.; Péchy, P.; Mathieu, H. J.; Descouts, P.; Grätzel, M. Surface Modification of Titanium with Phosphonic Acid to Improve Bone Bonding Characterization by XPS and ToF-SIMS. *Langmuir* **2002**, *18*, 2582−2589.
(34) Perez-Romo, P.; Potvin, C.; Manoli, J. M.; Chehimi, M. M.; Djéga-Mariadassou, G. Phosphorus-Doped Molybdenum Oxynitrides and Oxygen-Modified Molybdenum Carbides: Synthesis, Characterization, and Determination of Turnover Rates for Propene Hydrogenation. *J. Catal.* **2002**, *208*, 187−196.
(35) Jaewoo, K.; Sol, L.; Duckbong, S.; Young-Soo, S. Synthesis of Multiwall Boron Nitride Nanotubes Dependent on Crystallographic Structure of Boron. *Mater. Chem. Phys.* **2012**, *137*, 182−187.
(36) Sugino, T.; Tai, T.; Etou, Y. Synthesis of Boron Nitride Film with Low Dielectric Constant for Its Application to Silicon Ultralarge Scale Integrated Semiconductors. *Diamond Relat. Mater.* **2001**, *10*, 1375−1379.
(37) Sainsbury, T.; Ikuno, T.; Okawa, D.; Pacilé, D.; Fréchet, J. M. J.; Zettl, A. Self-Assembly of Gold Nanoparticles at the Surface of Amine- and Thiol-Functionalized Boron Nitride Nanotubes. *J. Phys. Chem. C* **2007**, *111*, 12992−12999.
(38) Vassileva, P.; Krastev, V.; Lakov, L.; Peshev, O. XPS Determination of the Binding Energies of Phosphorus and Nitrogen in Phosphazenes. *J. Mater. Sci.* **2004**, *39*, 3201−3202.
(39) Allcock, H. R.; Taylor, J. P. Phosphorylation of Phosphazenes and Its Effects on Thermal Properties and Fire Retardant Behavior. *Polym. Eng. Sci.* **2000**, *40*, 1177−1189.
(40) Dieck, R. L.; Quinn, E. J. Low Smoke Polyphosphazene Compositions. U. S. Patent 4083820, 1978.
(41) Reynard, K. A.; Rose, S. H. Flame-Retardant Poly-(Aryloxyphosphazene) Copolymers. U. S. Patent 3883451, 1975.
(42) Mueller, W. B. Polyphosphazene Form—A New Highly Fire Resistant Thermal Insulation. *J. Cell. Plast.* **1986**, *22*, 53−63.
(43) Anderson, D. R. Thermal Conductivity of Polymers. *Chem. Rev.* **1966**, *66*, 677−690.
(44) *Reaction-to-Fire Tests—Heat Release, Smoke Production and Mass Loss Rate—Part 1: Heat Release Rate (Cone Calorimeter Method)*, ISO 5660-1:2002; International Organization for Standardization: Geneva, Switzerland, 2002.
(45) Tang, Y.; Hu, Y.; Wang, S. F.; Gui, Z.; Chen, Z.; Fan, W. C. Preparation and Flammability of Ethylene-Vinyl Acetate Copolymer/Montmorillonite Nanocomposites. *Polym. Degrad. Stab.* **2002**, *78*, 555−559.
(46) Morgan, A. B.; Chu, L. L.; Harris, J. D. A Flammability Performance Comparison between Synthetic and Natural Clays in Polystyrene Nanocomposites. *Fire Mater.* **2005**, *29*, 213−219.
(47) Peeterbroeck, S.; Laoutid, F.; Swoboda, B.; Lopea-Cuesta, J. M.; Moreau, N.; Nagy, J. B.; Alexandre, M.; Dubois, P. How Carbon Nanotube Crushing Can Improve Flame Retardant Behaviour in Polymer Nanocomposites? *Macromol. Rapid Commun.* **2007**, *28*, 260−264.
(48) Laachachi, A.; Cochez, M.; Leroy, E.; Gaudon, P.; Ferriol, M.; Lopea-Cuesta, J. M. Effect of Al_2O_3 and TiO_2 Nanoparticles and APP on Thermal Stability and Flame Retardance of PMMA. *Polym. Adv. Technol.* **2006**, *17*, 327−334.
(49) Zhang, Z. Y.; Yuan, L.; Liang, G. Z.; Gu, A. J.; Qiang, Z. X.; Yang, C. W.; Chen, X. X. Unique Hybridized Carbon Nanotubes and Their High Performance Flame Retarding Composites with High Smoke Suppression, Good Toughness, and Low Curing Temperature. *J. Mater. Chem. A* **2014**, *2*, 4975−4988.
(50) Hirschler, M. M. In *Heat Release in Fires*; Babrauskas, E. V., Grayson, S. J., Eds.; Elsevier: London, 1992; Chapter 12a, pp 375−422.

(51) Stark, N. M.; White, R. H.; Mueller, S. A.; Osswald, T. A. Evaluation of Various Fire Retardants for Use in Wood Flour-Polyethylene Composites. *Polym. Degrad. Stab.* **2010**, *95*, 1903−1910.
(52) Liu, R.; Wang, X. D. Synthesis, Characterization, Thermal Properties and Flame Reatrdancy of a Novel Nonflammable Phosphazene-Based Epoxy Resin. *Polym. Degrad. Stab.* **2009**, *94*, 617−624.
(53) Vlaev, L. T.; Markovska, I. G.; Lyubchev, L. A. Non-Isothermal Kinetics of Pyrolysis of Rice Husk. *Thermochim. Acta* **2003**, *406*, 1−7.
(54) Zhuo, D. X.; Gu, A. J.; Liang, G. Z.; Hu, J. T.; Yuan, L.; Chen, X. X. Very Efficient Flame Retardancy Materials Based on a Novel Fully End-Capped Hyperbranched Polysiloxane and Bismaleimide/Diallylbisphenol A Resin with Simultaneously Improved Integrated Performance. *J. Mater. Chem.* **2011**, *21*, 6584−6594.
(55) Kissinger, H. E. Reaction Kinetics in Differential Thermal Analysis. *Anal. Chem.* **1957**, *29*, 1702−1706.
(56) Chen, Y. H.; Liu, Y.; Wang, Q.; Yin, H.; Aelmans, N.; Kierkels, R. Performance of Intumescent Flame Retardant Master Batch Synthesized Through Twin-Screw Reactively Extruding Technology: Effect of Component Ratio. *Polym. Degrad. Stab.* **2003**, *81*, 215−224.
(57) Baraton, M. I.; Merle, T.; Quintard, P.; Lorenzelli, V. Surface Activity of a Boron Nitride Powder: A Vibrational Study. *Langmuir* **1993**, *9*, 1486−1491.
(58) Dibandjo, P.; Bois, L.; Chassagneux, F.; Cornu, D.; Letoffe, J. M.; Toury, B.; Babonneau, F.; Miele, P. Synthesis of Boron Nitride with Ordered Mesostructure. *Adv. Mater.* **2005**, *17*, 571−574.
(59) Yang, C. W.; Liang, G. Z.; Gu, A. J.; Yuan, L. Flame Retardancy and Mechanism of Bismaleimide Resins Based on a Unique Inorganic-Organic Hybridized Intumescent Flame Retardant. *Ind. Eng. Chem. Res.* **2013**, *52*, 15075−15087.
(60) Xu, T.; Huang, X. M. A TG-FTIR Investigation into Smoke Suppression Mechanism of Magnesium Hydroxide in Asphalt Combustion Process. *J. Anal. Appl. Pyrolysis* **2010**, *87*, 217−223.
(61) Chen, X. L.; Zhuo, J. L.; Jiao, C. M. Thermal Degradation Characteristics of Flame Retardant Polylactide Using TG-IR. *Polym. Degrad. Stab.* **2012**, *97*, 2143−2147.
(62) Chen, X. L.; Huo, L. L.; Jiao, C. M.; Li, S. X. TG-FTIR Characterization of Volatile Compounds from Flame Retardant Polyurethane Foams Materials. *J. Anal. Appl. Pyrolysis* **2013**, *100*, 186−191.
(63) Tai, Q. L.; Yuen, R. K. K.; Yang, W.; Qiao, Z. H.; Song, L.; Hu, Y. Iron−Montmorillonite and Zinc Borate as Synergistic Agents in Flame-Retardant Glass Fiber Reinforced Polyamide 6 Composites in Combination with Melamine Polyphosphate. *Composites, Part A* **2012**, *43*, 415−422.
(64) Pramoda, K. P.; Liu, T. X.; Liu, Z. H.; He, C. B.; Sue, H. J. Thermal Degradation Behavior of Polyamide 6/Clay Nanocomposites. *Polym. Degrad. Stab.* **2003**, *81*, 47−56.
(65) Tai, Q. L.; Hu, Y.; Yuen, R. K. K.; Song, L.; Lu, H. D. Synthesis, Structure−Property Relationships of Polyphosphoramides with High Char Residues. *J. Mater. Chem.* **2011**, *21*, 6621−6627.
(66) Wu, K.; Zhang, Y. K.; Zhang, K.; Shen, M. M.; Hu, Y. Effect of Microencapsulation on Thermal Properties and Flammability Performance of Epoxy Composite. *J. Anal. Appl. Pyrolysis* **2012**, *94*, 196−201.
(67) Xu, J. Z.; Ma, R.; Jiao, Y. H.; Xie, J. X.; Wang, R.; Su, L. Synthesis, Characterization, and Thermal Degradation Property of Aniline Polyphosphazene. *J. Macromol. Sci, Part B: Phys.* **2011**, *50*, 897−906.
(68) Gouri, M. E.; Bachiri, A. E.; Hegazi, S. E.; Rafik, M.; Harfi, A. E. Thermal Degradation of a Reactive Flame Retardant Based on Cyclotriphosphazene and Its Blend with DGEBA Epoxy Resin. *Polym. Degrad. Stab.* **2009**, *94*, 2101−2106.